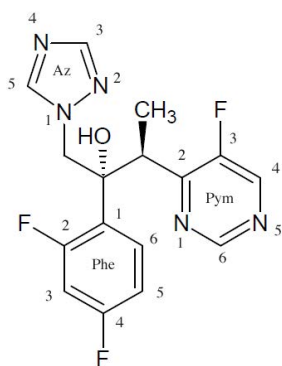


# Application of HFX NMR to Facilitate the Complete Assignment of the Anti-fungal Agent Voriconazole

## INTRODUCTION

Fluorine is found with an ever-increasing frequency in materials science and both legal and illicit drugs [ref 1-5]. In this application note results are presented to illustrate the simplification afforded by the routine application of triple-resonance NMR to clearly assign voriconazole, a molecule containing proton, carbon, and nitrogen molecules with many atoms exhibiting J-coupling to fluorine. The HFX ROYAL probe is a completely new probe technology utilizing magnetic coupling to afford highly efficient HF-X tuning which can function as a simple switch to highest sensitivity dedicated  $^1\text{H}$  or  $^{19}\text{F}$  or very well balanced dual  $^1\text{H}/^{19}\text{F}$  performance on demand. References 6-8 detail the technological developments for the HFX ROYAL probe.



Voriconazole

**Figure 1.** Structure of the anti-fungal voriconazole with a simplified numbering system. For example Pym 3 would refer to the fluorine-containing carbon of the pyrimidine ring.

The  $^1\text{H}$  NMR spectrum acquired at 500 MHz with the Royal HFX probe using the ECZR 500 console is presented in figure 2. Because of the nature of the structure there is at first glance very little fine structure to facilitate clear assignments. Almost all resonances including what appear to be singlets are significantly sharpened by the application of  $^{19}\text{F}$  decoupling. However, the top pane of figure 2 detailing the phenyl region which contains two  $^{19}\text{F}$  resonances cannot be visually assigned without  $^{19}\text{F}$  decoupling. Decoupling  $^{19}\text{F}$  removes confusion with the three resonances for Phe-6, Phe-3, and Phe-5 being revealed with classically simple ortho, ortho-meta, and meta coupling patterns respectively... cannot be visually assigned without  $^{19}\text{F}$  decoupling.

In figure 2 we see a simple illustration for how  $^{19}\text{F}$  can interact with the  $^1\text{H}$  spectrum but far more information is easily available to actually map out which specific  $^{19}\text{F}$  species are interacting with which  $^1\text{H}$  resonances. NMR pulse sequences such as HFHETCOR or HFCOSY allow H-F connectivity to be mapped in two dimensions. Figure 3 shows the HFCOSY 2D result obtained for Voriconazole.

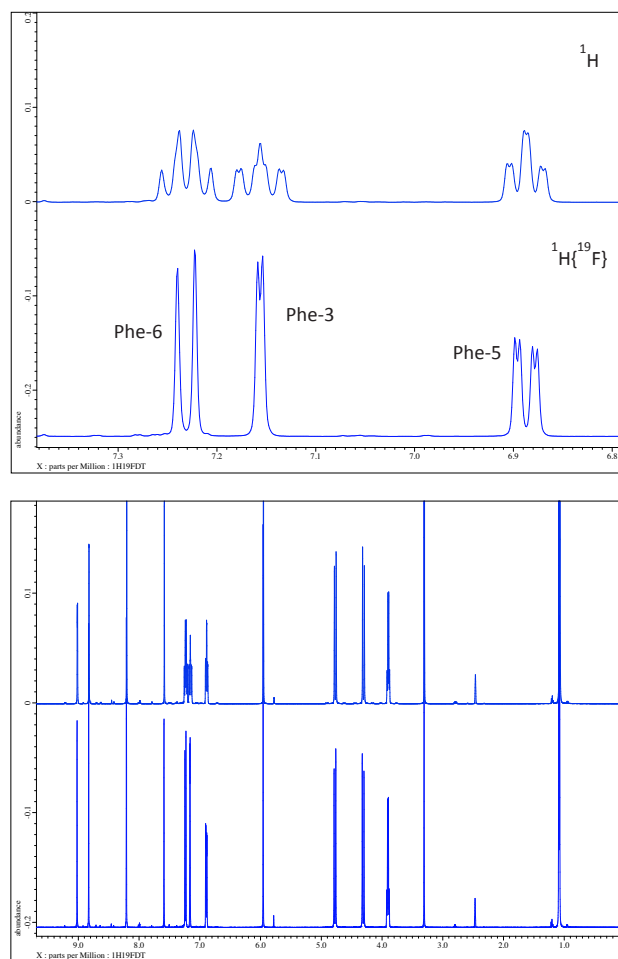


**Figure 2.**  $^1\text{H}$  NMR spectrum of Voriconazole with and without  $^{19}\text{F}$  decoupling. Bottom pane - full spectrum; top pane - expansion of the region revealing how the coupling details of the phenyl group are clarified by  $^{19}\text{F}$  decoupling.

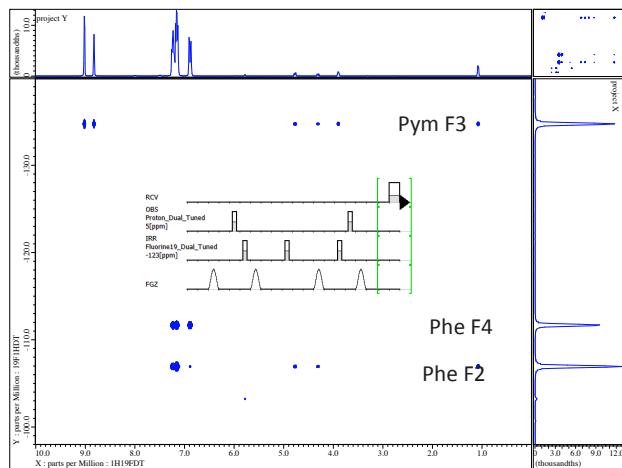


Figure 3. HF-COSY for Voriconazole mapping connectivity between protons and fluorines.

A very powerful feature in this particular example is the fact that taking the simple 1D proton results from figure 2 into account where the 3 phenyl protons are easily assigned by the  $^1\text{H}$  NMR coupling patterns the HF-COSY now allows unambiguous assignment of each  $^{19}\text{F}$  molecule in voriconazole. In addition the HF-COSY reveals by way of the observed responses into the  $^1\text{H}$  spectrum the singlets which are H-4 and H-6 in the pyrimidine ring. It is not yet possible to assign which singlet in the 8.8-9.0ppm region is Pym H-4 or Pym H6 so further experiments will be necessary.

This is a good time to introduce the interactions between  $^{19}\text{F}$  upon the  $^{13}\text{C}$  NMR spectrum. In figure 4 a significant signal enhancement and simplification can be seen for the  $^{13}\text{C}$  spectrum brought about by the dual decoupling of  $^1\text{H}$  &  $^{19}\text{F}$  as opposed to only decoupling  $^1\text{H}$ . By simply comparing the  $^{13}\text{C}$  spectra with only  $^1\text{H}$  decoupling to a spectrum with dual  $\{^1\text{H } ^{19}\text{F}\}$  decoupling all carbons with attached  $^{19}\text{F}$  atoms now become apparent. In addition all  $^{19}\text{F}/^{13}\text{C}$  coupling constants can be extract by simple inspection. Note that actual assignments cannot be made quite yet but it should be apparent that access to  $^1\text{H}/^{19}\text{F}$  and now  $^{13}\text{C}\{^1\text{H } ^{19}\text{F}\}$  data has easily provided quite a bit of information in addition to the sensitivity enhancements.

At this point in the assignment process it is time to introduce heteronuclear experiments involve all three nuclei,  $^1\text{H}$ ,  $^{13}\text{C}$  and  $^{19}\text{F}$ . While any 2 or 3 dimensional combination is possible we will focus on the higher sensitivity experiments which correlate either  $^1\text{H}$  or  $^{19}\text{F}$  to  $^{13}\text{C}$  with application of respectively either  $^{19}\text{F}$  or  $^1\text{H}$  decoupling in all dimensions. The 1-bond HSQC-based correlation experiments are of course purely bookkeeping in nature by allowing a simple mapping of directly connected protons or fluorines to  $^{13}\text{C}$ . For cases where any of the assignments of an individual species are known it allows assignment of the directly connected partner by simple inspection.

To this point we have only actually assigned the 3 fluorine atoms (via the HF-COSY and simple  $^{19}\text{F}$  decoupled  $^1\text{H}$  spectrum) the 3 protons in the phenyl ring. Thus,  $^1\text{H}/^{13}\text{C}$  HSQC would provide all directly correlated H-C pairs and transfer the assignments for protons Phe6, Phe3, & Phe5 to the carbon partners. In addition

the multiplicity-edited HSQC would allow confirmation of the rather obvious assignments for the OH (missing in HSQC) and the aliphatic CH,  $\text{CH}_2$  and  $\text{CH}_3$  species. The  $^1\text{H}/^{13}\text{C}\{^{19}\text{F}\}$  edited C2HSQC result for voriconazole is shown in figure 5.

Of further interest in figure 5 the lone aliphatic CH carbon is found near 40ppm which was completely obscured by the  $\text{DMSO}_d_6$  solvent in the 1D carbon NMR spectrum in figure 4.

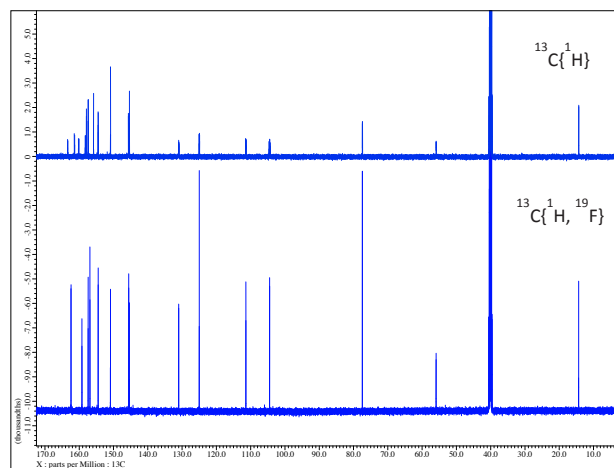
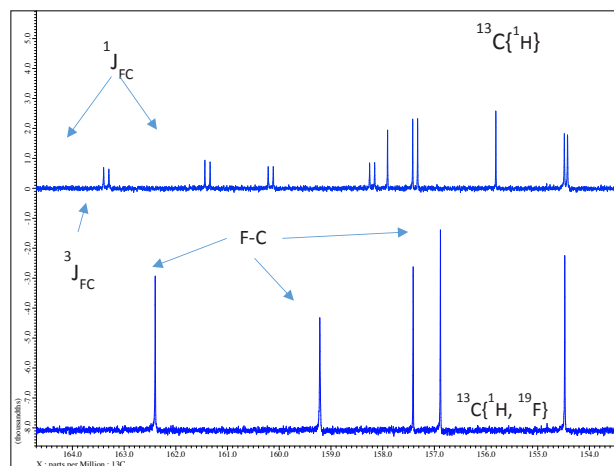


Figure 4. Comparison of 1D  $^{13}\text{C}$  NMR spectrum for voriconazole comparing effects of  $^1\text{H}$  decoupling and dual  $\{^1\text{H } ^{19}\text{F}\}$  decoupling. The top pane better illustrates the profound simplifications from  $\{^1\text{H } ^{19}\text{F}\}$ .

Before proceeding to the  $^{19}\text{F}/^{13}\text{C}\{^1\text{H}\}$  C2HSQC experiment it is important to provide a few details regarding the choice of C2HSQC [ref 9] for this work. C2HSQC utilizes short BIP inversion pulses for both  $^{13}\text{C}$  and  $^{19}\text{F}$  180 degree pulses. In reference 9 the authors clearly illustrate the large increase in performance which is obtained by use of doubly compensated multiplicity-edited HSQC experiments compared to single compensation, or simple square pulse experiments. This is because the bandwidth required for  $^{13}\text{C}$ , and especially  $^{19}\text{F}$ , simply renders to use of simple square 180 pulses as nearly useless. The choice of BIP inversion pulses [ref 10] in tailored pairs to effect refocusing is also advantageous because of the very large  $^{19}\text{F}/^{13}\text{C}$  coupling constants (260 - 280 Hz) which provides very little time for the  $1/(2^*J)$  required for INEPT transfer.

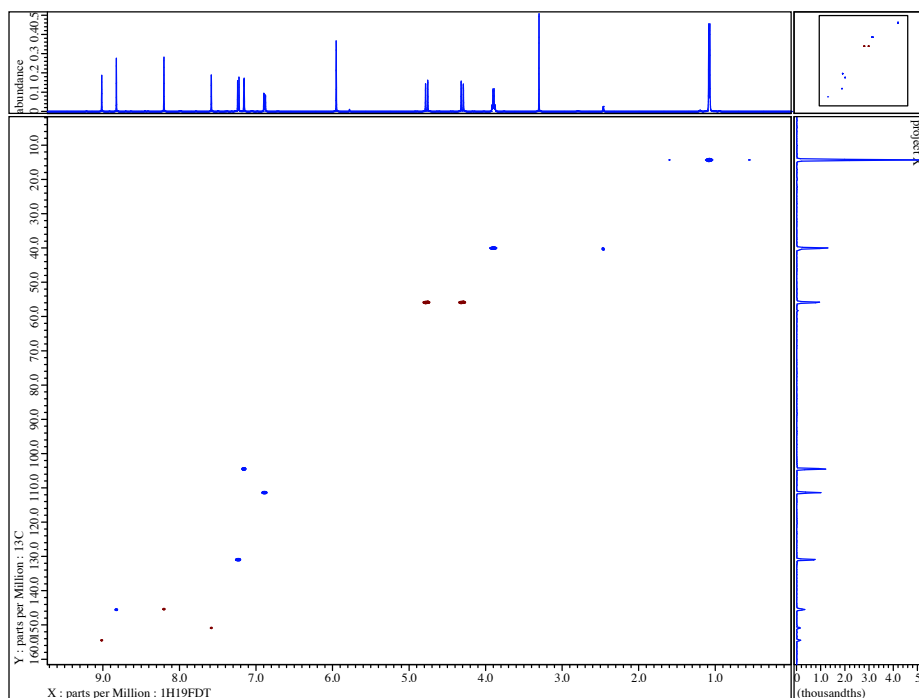


Figure 5.  $^1\text{H}$  detected  $^{13}\text{C}$  C2HSQC with full  $^{19}\text{F}$  decoupling in both dimensions. Note the absence of a correlation for the  $^1\text{H}$  singlet near 6ppm assigning it as the OH. Also note the pair of protons near 4.4 & 4.8 ppm are connected to a single carbon near 56ppm allowing assignment as the lone N-CH<sub>2</sub> carbon attached to the triazole ring. In addition the previously assigned phenyl protons between 6.8 and 7.4ppm reveal their carbon attachments.

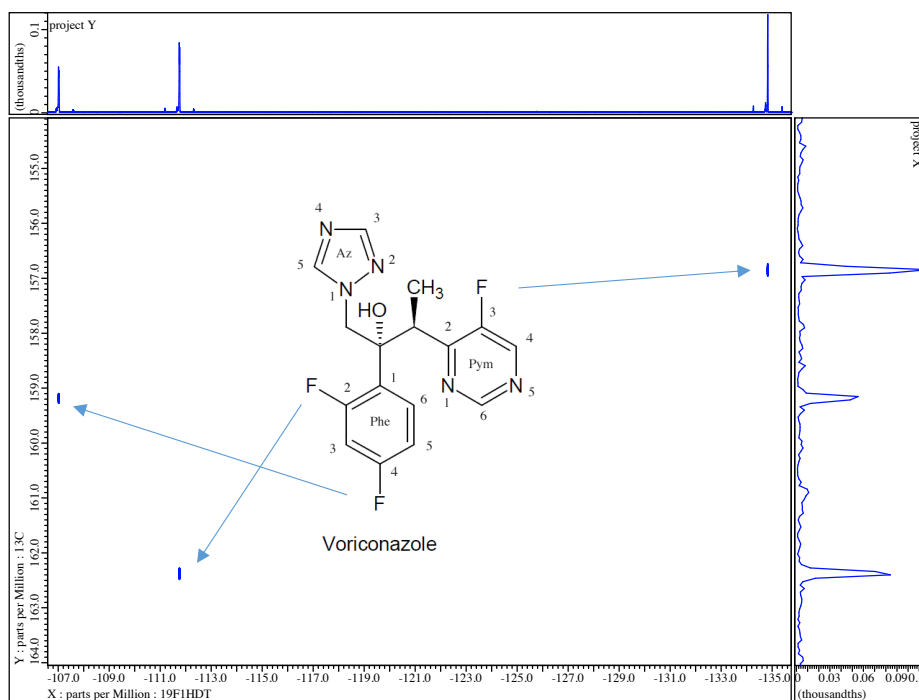


Figure 6. Fully F1/F2  $\{^1\text{H } ^{13}\text{C}\}$  decoupled  $^{19}\text{F}/^{13}\text{C}$  c2hsqc. Voriconazole in  $\text{DMSO-d}_6$ . Simple inspection of the data allows transfer of the known assignments for the 3 fluorine resonances to their directly attached carbons.

In table 1 we will list all resonance chemical shifts for  $^1\text{H}$ ,  $^{13}\text{C}$ , and  $^{19}\text{F}$  and list all assignments to this point. So far as  $^1\text{H}$ ,  $^{13}\text{C}$  and  $^{19}\text{F}$  are concerned everything is assigned except for the 2 CH resonances in both the triazole and pyrimidine rings and the 2 aromatic quaternary carbons. To complete the assignments as well as add the 5  $^{15}\text{N}$  resonances we must employ long range heteronuclear connectivity experiments.

$^{13}\text{C}$	$^1\text{H}$	$^{19}\text{F}$	Multiplicity	Assign
162.37	--	-111.76	CF	Phe4
159.19	--	-107.02	CF	Phe2
157.37	--	--	quat	?
156.86	--	-134.83	CF	Pym3
154.46	9.015	--	CH	?
150.87	7.585	--	CH	?
145.55	8.824	--	CH	?
145.36	8.202	--	CH	?
130.96	7.231	--	CH	Phe6
124.97	--	--	quat	?
111.38	6.892	--	CH	Phe5
104.46	7.157	--	CH	Phe3
77.4	--	--	quat	C-OH
55.89	4.774;4.304	--	CH2	CH2 at triazole N1
40.06	3.899	--	CH	CH-with CH3
14.32	1.079	--	CH3	CH3
--	5.95	--	OH	OH

Table 1. Summary list of assignments allowed by simple inspection of the 1D NMR spectra, the HFCOSY and  $^1\text{H}/^{13}\text{C}$   $^{19}\text{F}/^{13}\text{C}$  c2hsqc 2D experiments.

The gHMBCAD pulse sequence [ref 11] was used to acquire  $^1\text{H}/^{13}\text{C}$   $\{^{19}\text{F}\}$  and  $^{19}\text{F}/^{13}\text{C}$   $\{^1\text{H}\}$  long-range correlation experiments to complete the missing  $^1\text{H}$  &  $^{13}\text{C}$  assignments. In addition  $^1\text{H}/^{15}\text{N}$   $\{^{19}\text{F}\}$  and  $^{19}\text{F}/^{15}\text{N}$   $\{^1\text{H}\}$  data was acquired to assign the 5 nitrogens in voriconazole.

Note that with just a quick inspection of the gHMBCAD in figure 7 we can now assign the quaternary carbons Pym2 and Ph1 as well as the rather obvious aliphatic quaternary carbon to which the OH is attached. Furthermore we also now clearly know which of the 4 aromatic singlets are associated with both the triazole and pyrimidine rings though we cannot yet say for the case of the pyrimidine which is H4 and which is H6 or for the triazole which is H3 and which is H5. Thus other than the ambiguity for Pym 4 & 6 and Az 3 & 5 we have completely and easily assigned voriconazole. Before we resolve these ambiguities by  $^1\text{H}/^{15}\text{N}$  gHMBCAD we will explore the effects of decoupling  $^{19}\text{F}$  in  $^1\text{H}/^{13}\text{C}$  gHMBCAD.

In figure 8 we compare  $^1\text{H}/^{13}\text{C}$  gHMBCAD for the small boxed region in figure 7. Note the large simplification resulting from decoupling  $\{^{19}\text{F}\}$  in both dimensions. Now it is time to move to  $^1\text{H}/^{15}\text{N}$  gHMBCAD in figures 9 & 10 and see how easily we can resolve the ambiguity for the 2 pairs of singlets in the pyrimidine and triazole rings.

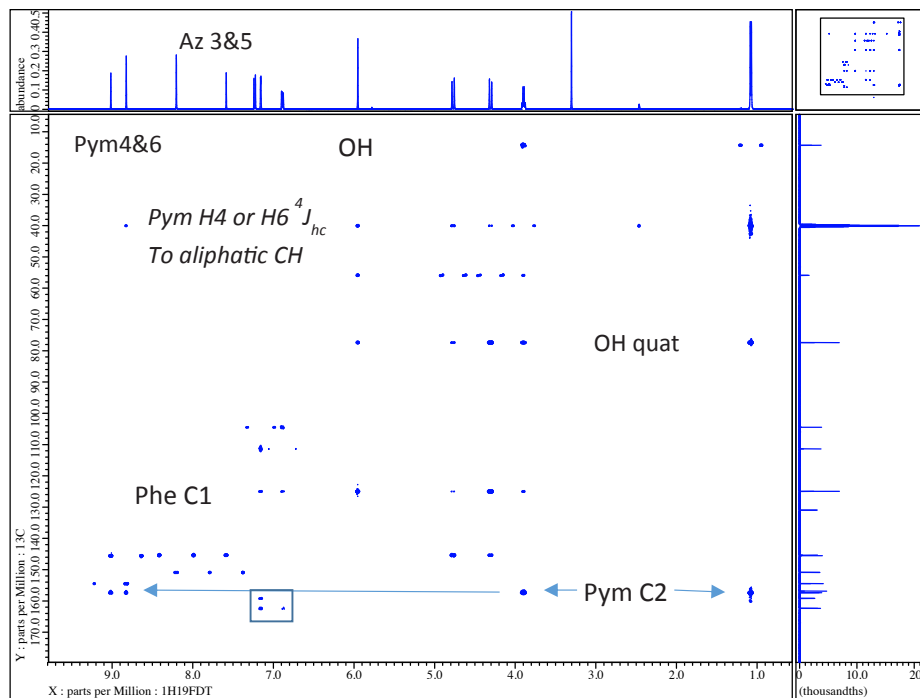


Figure 7. Fully  $\{^{19}\text{F}\}$  decoupled  $^1\text{H}/^{13}\text{C}$  gHMBCAD. Data was acquired with the low pass filter deliberately unmatched to the directly attached protons to retain weak  $^1\text{J}$  responses as a small aid to making assignments without reference to the HSQC. Note the cleanly  $\{^{19}\text{F}\}$  decoupled responses within the boxed area which involve the pyrimidine carbons 2 & 4 attached to  $^{19}\text{F}$ .

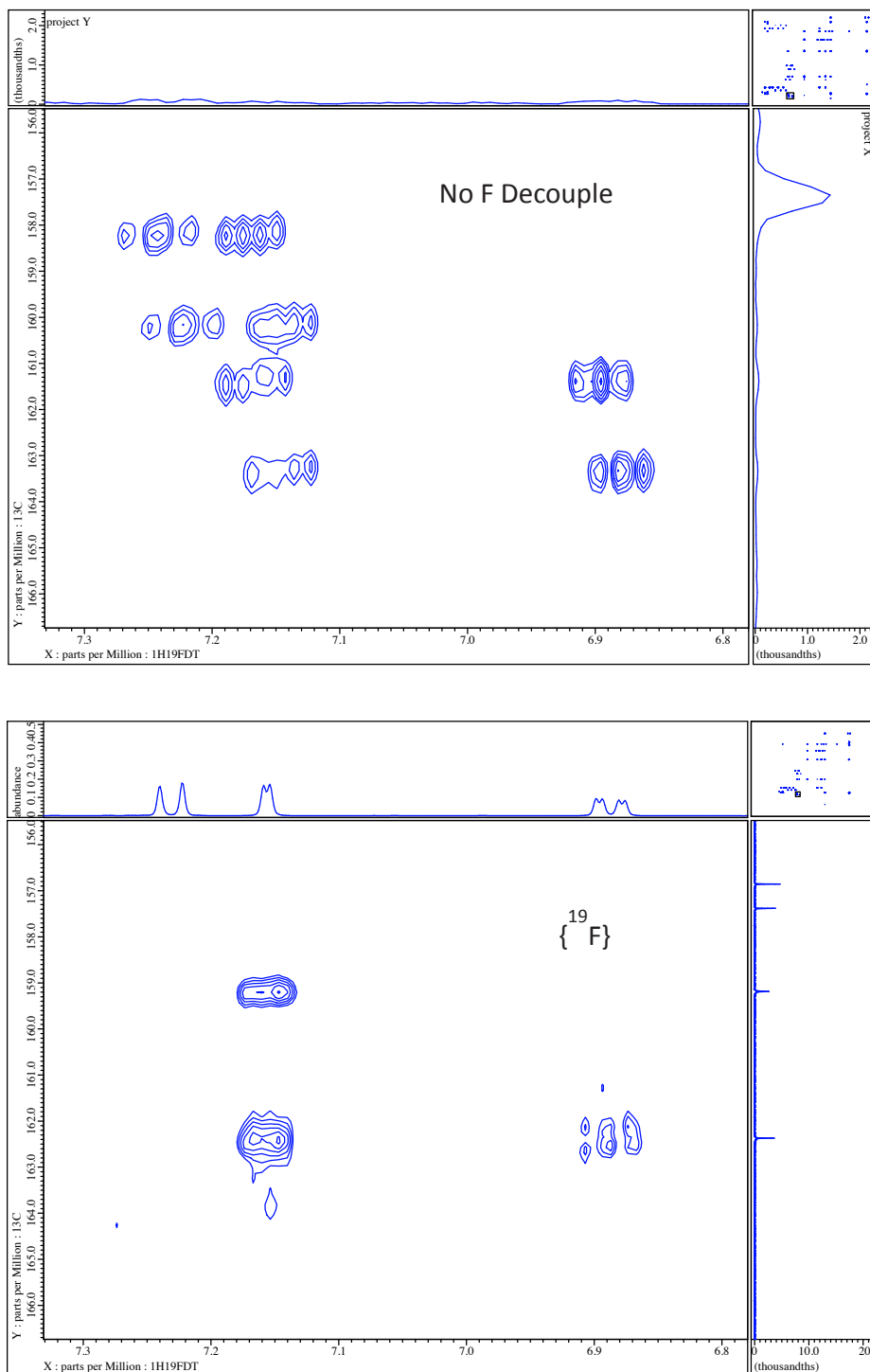


Figure 8. Comparison of  $^1\text{H}/^{13}\text{C}$  gHMBCAD without (top) and with (bottom)  $\{^{19}\text{F}\}$  decoupling. Note that the pane on the bottom was acquired in 1/4<sup>th</sup> the time of the non-decoupled data on the top.

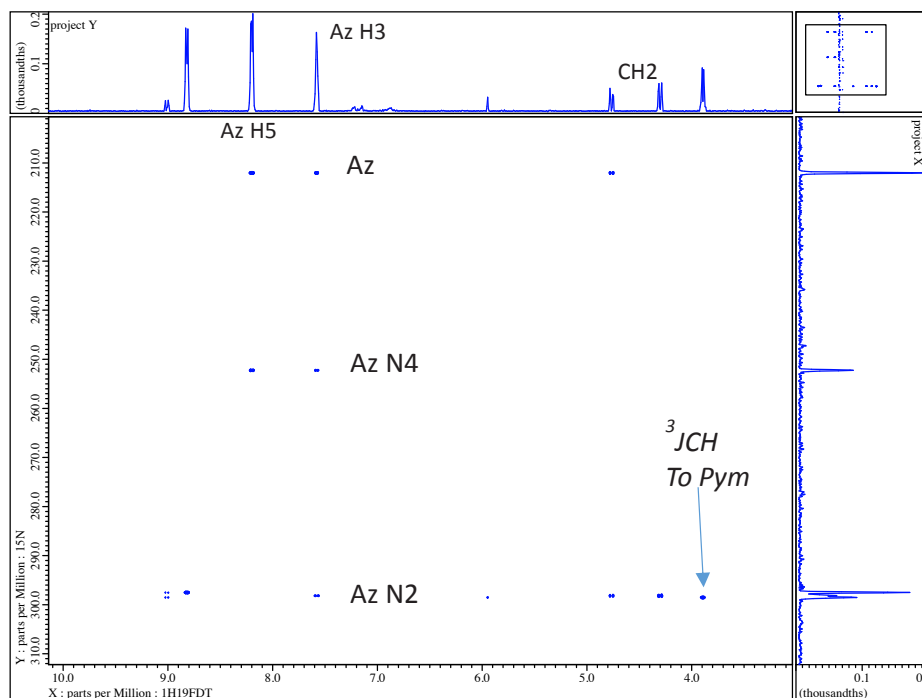


Figure 9. Fully  $\{^{19}\text{F}\}$  decoupled  $^1\text{H}/^{15}\text{N}$  gHMBCAD. Because the unusual situation of 3  $^{15}\text{N}$  resonances occurring between 297 and 299 ppm a detailed expansion is shown as figure 10.

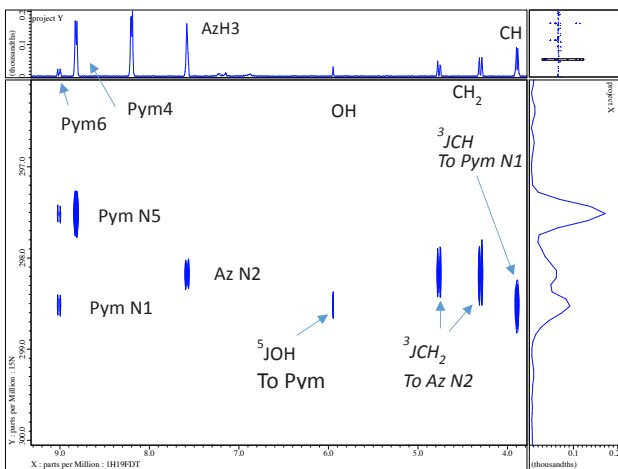


Figure 10. Detailed expansion of the 297 - 299 ppm region of the fully  $\{^{19}\text{F}\}$  decoupled  $^1\text{H}/^{15}\text{N}$  gHMBCAD completing all assignments.

$^{13}\text{C}$	$^1\text{H}$	$^{19}\text{F}$	Multiplicity	Assign
162.37	--	-111.76	CF	Phe4
159.19	--	-107.02	CF	Phe2
157.37	--	--	quat	Pym2
156.86	--	-134.83	CF	Pym3
154.46	9.015	--	CH	Pym4
150.87	7.585	--	CH	Az3
145.55	8.824	--	CH	Pym6
145.36	8.202	--	CH	Az5
130.96	7.231	--	CH	Phe6
124.97	--	--	quat	Phe1
111.38	6.892	--	CH	Phe5
104.46	7.157	--	CH	Phe3
77.4	--	--	quat	C-OH
55.89	4.774; 4.304	--	CH <sub>2</sub>	CH <sub>2</sub> at triazole N1
40.06	3.899	--	CH	CH-with CH <sub>3</sub>
14.32	1.079	--	CH <sub>3</sub>	CH <sub>3</sub>
--	5.95	--	OH	OH
		$^{15}\text{N}$		
		299.91		AZ2
		298.52		Pym1
		297.52		Pym5
		252.18		Az4
		211.99		Az1

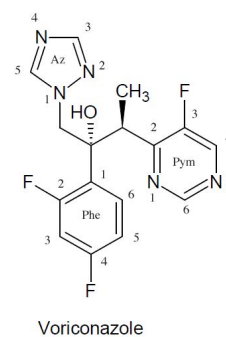


Table 2. Summary list of all assignments for voriconazole for all  $^1\text{H}$ ,  $^{13}\text{C}$ ,  $^{19}\text{F}$ , &  $^{15}\text{N}$  resonances.

At this point we have achieved the goal of completely assigning all resonances for the voriconazole sample but have the luxury being able to now employ  $^{19}\text{F}/^{13}\text{C}$  and  $^{19}\text{F}/^{15}\text{N}$  gHMBCAD with full  $\{^1\text{H}\}$  decoupling as a completely independent check of many of the assignments. The  $^{19}\text{F}/^{13}\text{C}$  gHMBC is shown in figure 11 and the  $^{19}\text{F}/^{15}\text{N}$  gHMBCAD in figure 12.

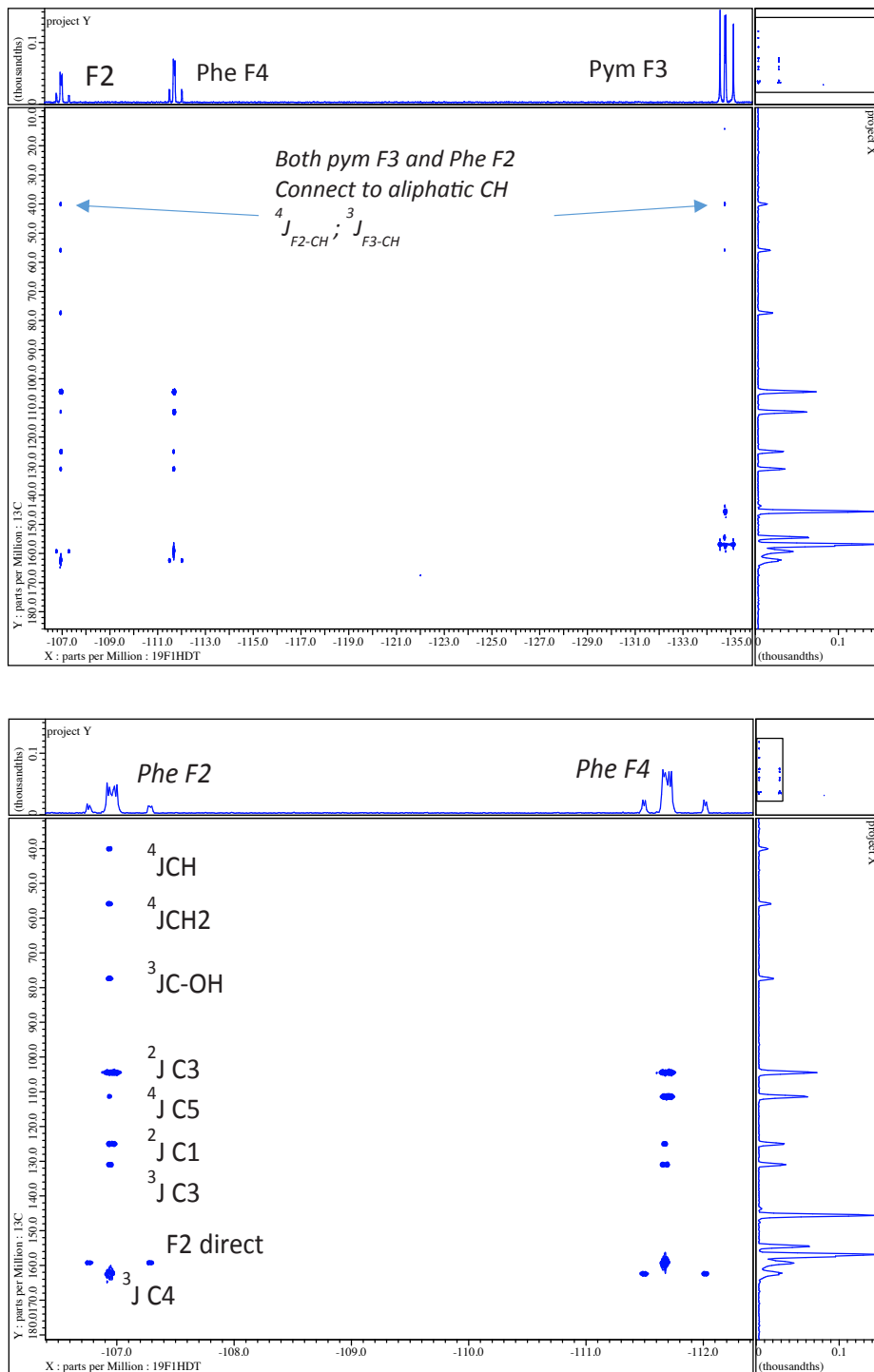


Figure 11.  $^{19}\text{F}/^{13}\text{C}$  gHMBCAD with full  $\{^1\text{H}\}$  decoupling. Top pane is full spectral window and bottom pane shows an expanded region.

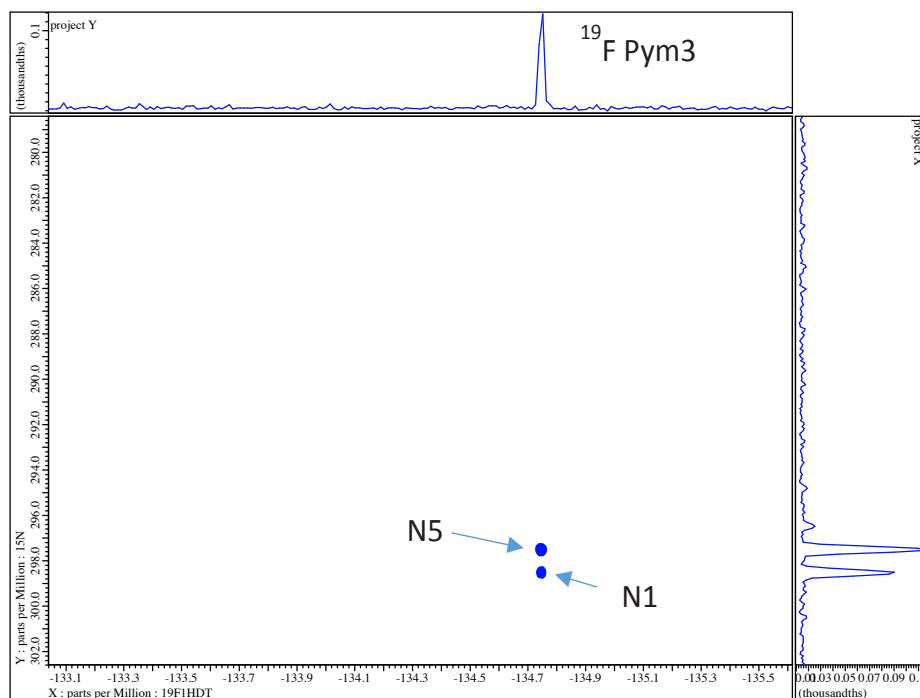


Figure 12.  $^{19}\text{F}/^{15}\text{N}$  gHMBCAD with full  $\{^1\text{H}\}$  decoupling. The assignments of N5 & N1 of the pyrimidine ring are confirmed in a very clear and simple fashion.

## CONCLUSION

By using HF-X NMR in a variety of one and two-dimensional experiments it is possible to clearly assign all resonances in an important drug such as the chosen example of voriconazole. The HFX ROYAL NMR probe allows easy on-demand access to such an array of experiments in a full automation environment.

## REFERENCES

1. Wang et al, *Chem. Rev.* 2014, 114, p2432-2506
2. Zhou et al, *Chem. Rev.* 2016, 116, p422-518
3. <http://www.slweb.org/ftrcfluorinatedpharm.html>
4. Banister et al, *ACS Chem. Neurosci.*, 2015, 6 (8), p1445-1458
5. Trachsel, D., *Drug Test. Analysis*, 2012, 4: p577-590
6. B. Taber and A.P. Zens, *J. Magn. Reson.*, 259, 2015, p114-120
7. P. Bowyer, J. Finnigan, B. Marsden, B. Taber, and A. Zens, *J. Magn. Reson.*, 2015, p190-1
8. V. Lim, B. Marsden, B. Taber, and A. Zens, *J. Magn. Reson.*, 2016, p.268
9. H. Hu, K. Krishnamurthy, *Magn. Res. Chem.*, 46 issue 7, 2008, p 683-689
10. M. Smith, H. Hu, and A.J. Shaka, *J. Magn. Reson.*, 151, 2001, p 269-283
11. R. Crouch, R. Boyer, R. Johnson, and K. Krishnamurthy, *Magn. Reson. Chem.*, 42, 2004, p301-307